

An Extended Version of Transverse Wave Approach (TWA) for Full-Wave Investigation of Planar Structures

M. Ayari, T. Aguilu

Syscom Laboratory, Engineer National School- B.P 37 Le belvedere 1002 Tunis-Tunisia

Mohamed.ayari@esti.rnu.tn, Taoufik.aguilu@enit.rnu.tn

H. Temimi

Department of mathematics, Virginia Polytechnic Institute and state university-Blacksburg, Virginia 24061-0123

temimi@vt.edu

H. Baudrand

Recherches et Concepts en Electromagnétisme, RCEM, 17 Rue Denis Papin, 31500 Toulouse -France

Henri.baudrand@enseehit.fr

Abstract— An original transverse wave approach (TWA) is presented for full-wave investigation of planar structures in a periodic network. The introduction of a novel surface impedance sub-domain in TWA offers a natural framework for the implementation of complex planar circuits with simple layer. The simulation results given by our new electromagnetic software developed under C++ environment are in full agreement with the literature.

Index Terms— TWA, surface impedance, planar structures, simulation.

I. INTRODUCTION

Since more than one decade, electromagnetic simulation has made its entry in the field of design of the integrated circuit and provided for the simulators a large library incorporating the most complex and sensitive geometry elements.

The diversity of physical phenomena which met in the microwave frequency field for the study of planar structures makes impossible to circumvent a rigorous electromagnetic analysis.

Therefore, a great variety of EM simulation techniques for EM field modeling has been developed so as to tackle these problems. Solely, numerical EM methods are used because for many EM structures like antennas, active devices, electromagnetic interference (EMI), and RF and microwave circuits, exact analytical solutions cannot be found. It is therefore necessary to consider these approaches to obtain approximate solutions of field problems.

These numerical EM methods are either discrete methods requiring the space discretizations by limiting the computational domain [1-2] or integral methods refining the calculation algorithms [3-4].

The introduction of Hilbert space methods to transform integral formulations of EM field to problems into algebraic ones is the central component of our approach. Therefore, this approach named Transverse Wave Approach (TWA) is reestablished neither on electric fields nor on current

density but on linear combination between them in order to obtain simulation results of the required accuracy with a minimum of computational effort.

Furthermore, the study of the complex planar structures needs a high-resolution which increases the CPU computation time; therefore, we propose to change the boundary conditions by the introduction of the surface impedance notion in TWA so as to simplify the studied structure and enhance the performance of our approach.

In this article, we develop this new approach with walls of periodical nature (Fig.1). This type of walls is used not only to protect the RF components from the parasitic radiation but also opens a framework for the study of antenna networks; this box (perfect conductor) defines the basis of EM field also, it can be used as a mechanical support and a shielding for the studied structure [9]-[12].

Thus, no matrix inversion is required by the TWA and the convergence is insured independently of the interfaces of this structure. Moreover, no limitations on the shape of the components are imposed; in fact, the TWA handles bounded operators and circumvents the inversion of an integral operator in treating, in an iterative way, the integral relations in the spectral domain and the continuity conditions in the spatial domain. TWA properly distinguishes the topological characteristics of circuits from their embedding environment.

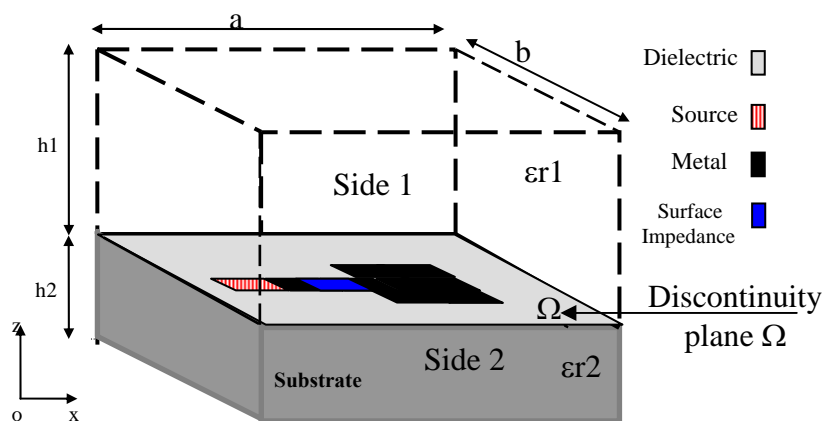


Fig .1. Schematic of a planar structure with simpler layer placed in a case bordered of periodic walls.

In the TWA approach, numerical instabilities related to matrices with large condition number (these matrices are poorly invertible and the accuracy of solution of a linear system may be bad), are circumvented by the introduction of the transverse waves instead of the tangential electromagnetic fields that allows us to handle scattering operators rather than manipulating unbounded impedance or admittance operators [1]-[7-8]. In section II, we present the theoretical background of the TWA and its extension to simple layer structures including the novel surface impedance sub-domain from the discontinuity plane (Fig.1) This type of field is used for decreasing the complexity degree on the level of the planar circuits, modeling the active circuits and simplifying the structures in multi-scale technology [1-2]-[5-6].

The contribution of the Fast Fourier Transform (FFT) in TWA and the implementation of this approach under C++ environment are developed in Section III. Some simulation results given by our electromagnetic software based on TWA with both dipole and fractal antennas are discussed in section IV.

II. THEORY

A. Wave concept

The wave concept is established by setting relations linking electromagnetic fields (electric field E_i and Current density J_i) to the reflected waves A_i and the incident waves B_i (from the discontinuity interface).

Let us call $\Omega_i, i \in \{1,2\}$: interfaces infinitely close to both sides of the interface Ω , with \vec{n}_i : normal vector directed towards region i (Fig. 2).

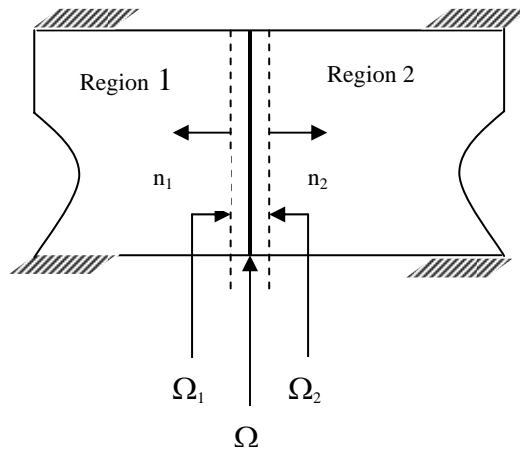


Fig .2. Discontinuity interfaces

The both incident (B_i) and reflected (A_i) waves are thus defined by:

$$\begin{aligned} \vec{A}_i &= \frac{1}{2\sqrt{Z_{0i}}} (\vec{E}_T^i - Z_{0i} * \vec{H}_T^i \times \vec{n}_i) \\ \vec{B}_i &= \frac{1}{2\sqrt{Z_{0i}}} (\vec{E}_T^i + Z_{0i} * \vec{H}_T^i \times \vec{n}_i) \end{aligned} \tag{1}$$

Where: $Z_{0i} = \sqrt{\frac{\mu_0}{\epsilon_0 \epsilon_r}}$ wave impedance from region i .

\vec{E}_T^i, \vec{H}_T^i : Transverse fields (Electric and magnetic)

B. TWA

The TWA approach uses equations easier to solve than the integral methods: there are no trial functions and no matrices inversions. Moreover, there is no geometric constraint [7]-[9-10]. The both reflected A_i and incident B_i waves are successively defined in the spectral and spatial domain, which constitute the iteration process. The toggling between the spatial and spectral wave expansions uses a mode-pixel transform readily based on fast Fourier transforms (FFTs).

1) FMT

To achieve this approach, the fast mode transform (FMT) is used to obtain the wave in the spectral domain from the one defined in the spatial domain. Moreover, the inverse fast mode transform (FMT-1) is the inverse operation according to the principle given by (Fig. 3).

The Parseval theorem is applied in each stage of the FMT in order to verify the energy conservation.

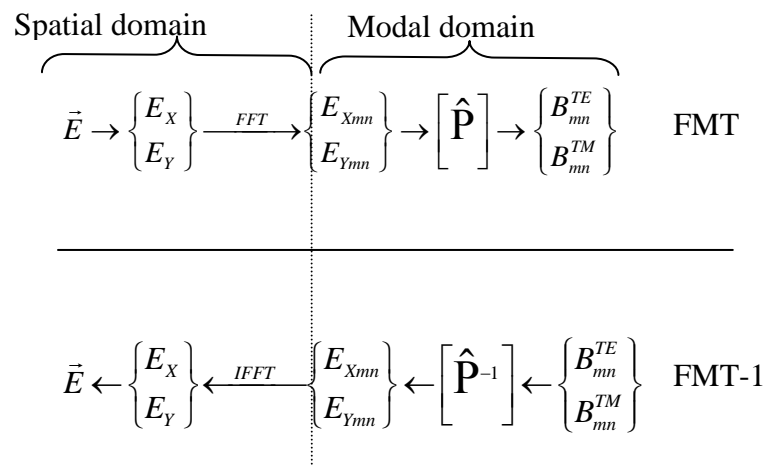


Fig .3. General principle of FMT (where [P]and [P-1] operators of passage between space and modal domain)

2) Iterative Resolution Process

On the one hand, the equations connecting the incident and reflected waves are as follows:

$$\begin{cases} \vec{A} = \hat{\Gamma} \vec{B} \\ \vec{B} = \hat{S} \vec{A} + \vec{B}_0 \end{cases} \quad (2)$$

Where: \vec{B}_0 denotes the global excitation wave on the source

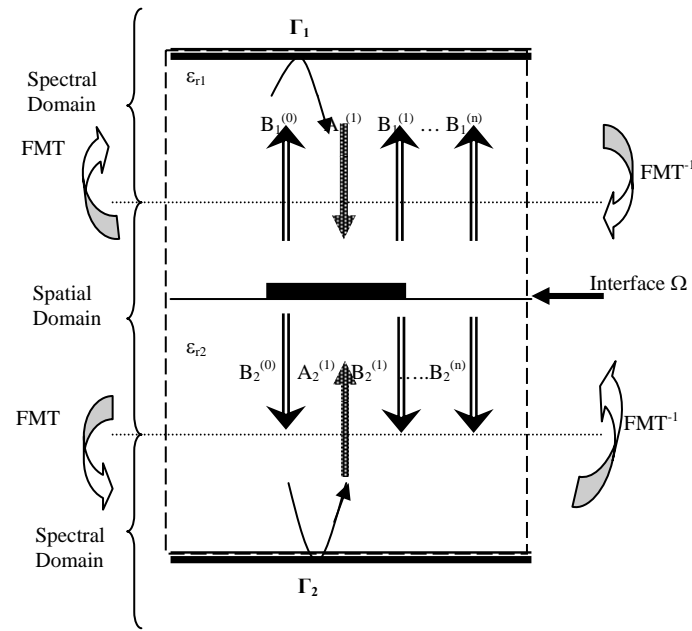


Fig. 4. Iterative process

OPERATOR $\hat{\Gamma}$

In the spectral domain, the modal expansion of the reflection operator following the Dirac notation is given by:

$$\hat{\Gamma} = \sum_{\alpha=TE,TM} \sum_m^{M_x} \sum_n^{M_y} |f_{m,n}^\alpha\rangle \Gamma_{m,n}^\alpha \langle f_{m,n}^\alpha| \tag{3}$$

Where $|f_{m,n}^{\alpha=TE,TM}\rangle$ are the transverse TE and TM eigen-functions of both the admittance and reflection operators verifying $\langle f_{p,q}^\alpha | f_{p',q'}^\alpha \rangle = \delta_{q,p'}^{p,q'}$ (the Kronecker symbol). $M_x \times M_y$ is the total number of TE and TM modes.

OPERATOR \hat{S}

\hat{S} is the spatial surface operator. It depends on the boundary conditions and therefore on the structure configuration. Generally, the air-dielectric interface (Ω) is divided into cells and includes three sub-domains dielectric (D), metal (M) and source (S):

The expressions of S on the three sub-domains are already given in [9-10].

A novel surface impedance sub-domain (I_{surf}) is introduced from discontinuity of plane (Ω) in order to reduce the complexity degree of planar structures. This sub-domain is characterized by complex impedance Zs.

The expression of S on I_{surf} is given by:

$$\hat{S} = \begin{bmatrix} \frac{Z_s(1-n^2) - Z_{01}}{Z_s(1+n^2) + Z_{01}} & \frac{2nZ_s}{Z_s(1+n^2) + Z_{01}} \\ \frac{2n.Z_s}{Z_s(1+n^2) + Z_{01}} & \frac{Z_s(n^2 - 1) - Z_{01}}{Z_s(1+n^2) + Z_{01}} \end{bmatrix} \quad (4)$$

Where $n = \frac{\sqrt{Z_{01}}}{\sqrt{Z_{02}}}$.

On the another hand, starting from the wave B0 excitation source, the TWA leads to an iterative scheme avoiding any operator inversion procedure to solve (2) as follows:

$$\begin{cases} \underline{\underline{B}}^{(0)} = \underline{\underline{B}}_0 \\ \underline{\underline{A}}^{(n)} = \hat{\Gamma} \underline{\underline{B}}^{(n-1)} \\ \underline{\underline{B}}^{(n)} = \hat{S} \underline{\underline{A}}^{(n)} + \underline{\underline{B}}_0 \end{cases} \quad (5)$$

Where (n) is the iteration order and the waves which are underlined in two features are presented in the domain space, the others in the domain modal.

All along the iterations, by successive reflections, the waves $\underline{\underline{A}}$ and B obey to:

$$\begin{cases} \Delta \underline{\underline{B}}^{(n)} = (\hat{S}\hat{\Gamma})^n \underline{\underline{B}}_0 \\ \Delta \underline{\underline{A}}^{(n)} = (\hat{\Gamma}\hat{S})^{n-1} \hat{\Gamma} \underline{\underline{B}}_0 \end{cases} \quad (6)$$

The convergence of (5) is reached when the norms $\|\Delta \underline{\underline{B}}^{(n)}\|$ and $\|\Delta \underline{\underline{A}}^{(n)}\|$ tend toward zero. The convergence speed is driven by the spectral radius of $\|\hat{S}\hat{\Gamma}\|$ and $\|\hat{\Gamma}\hat{S}\|$.

Let $\rho(\hat{U})$ be the spectral radius of operator \hat{U} then the convergence condition is established if:

$$\rho(\hat{U}) < 1 \quad (7)$$

The convergence of the TWA in (n) iterations can be observed on the input impedance $Z_{in}^{(n)}$ (or admittance $Y_{in}^{(n)}$) calculated on the source sub-domain as:

$$Z_{in}^{(n)} = \frac{\sum_{Source\ Sub-domain} E^{(n)} E^{(n)*}}{\sum_{Source\ Sub-domain} E^{(n)} (J_1^{(n)} + J_2^{(n)})^*} \times Form_Fact \quad (8)$$

where:

$J_i^{(n)}$: Current density in each region i at iteration (n).

$E^{(n)}$: Electric field in excitation side at iteration (n).

Form _ Fact: the form factor of excitation source.

III. IMPLEMENTATION OF THE TWA UNDER C++ ENVIRONMENT

A. Contribution of FFT compared with DFT during the implementation of TWA

After defining the grid resolution to the interface's discontinuity, the number of pixels along the x-axis and y-axis must all be powered by 2, likewise the number of TE and TM modes.

This condition on the grid comes from the FFT which is a faster version of the Discrete Fourier Transform (DFT). This acceleration is based on the *Danielson Lanczos* algorithm [11] which imposes that the selected number of points must all be powers of 2.

Although the FFT presents this disadvantage, it remains much more flexible in its implementation than that of the DFT even if the latter does not have any condition imposed on it. The table below proves this:

TABLE I. COMPARISON THE CPU COMPUTATION TIME OF SIMULATION BETWEEN DFT AND FFT

		Pixel number		
		32*32 pixels	64*64 pixels	128*128 pixels
DFT	Time (sec) 1 iteration	10	43	180
	Time(min) 100 iteration	16.7	71.7	300
FFT	Time (sec) 1 iteration	0.1	0.4	1.4
	Time(min) 100 iteration	0.16	0.67	2.3

The discrete Fourier transform can, in fact, be computed in $O(N \log_2 N)$ operations with an algorithm called the FFT. The difference between $N \log_2 N$ and N^2 is large. For example, for $N = 10^6$, there is a large difference between, 30 seconds of CPU time and 2 weeks of CPU time on a microsecond cycle time computer.

B. Electromagnetic simulation tool based on TWA

Based on the TWA, we developed an electromagnetic simulation tool under object oriented environment: C++. The choice of this environment is justified by the need for short time of calculation with a significant saving in resource's memories for the storage of data, which make available the analysis from the complex structures requiring a high precision of description. The general scheme of this tool is presented in Fig.5.

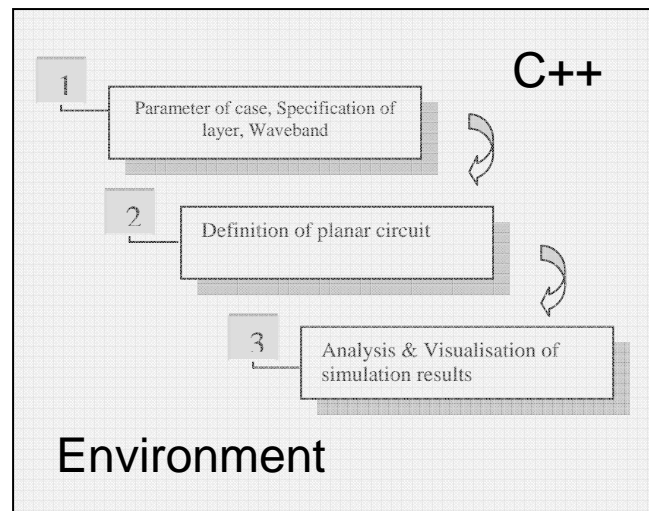


Fig. 5. Use case of the tool

Our simulation tool is composed of three modules: (1) presents the specification of physical proprieties of layer, dimension of case and investigation waveband, (2) defines the circuit and (3) analyses and visualizes the different simulation results. The detail of these modules is described in Fig. 6.

Detailed tree structure of tool:

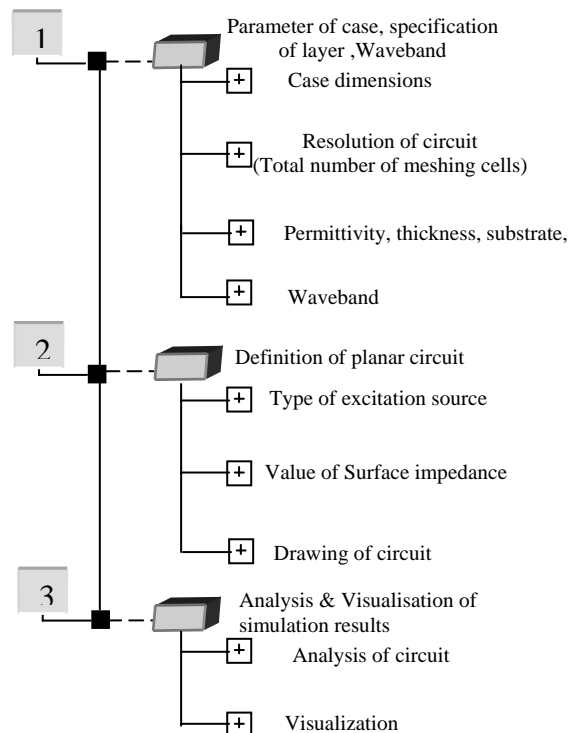


Fig. 6. Organization chart of different steps of specification, analysis and visualization of tool

IV. SIMULATIONS RESULTS

A. First Application example: Antenna dipole

1) Test structure

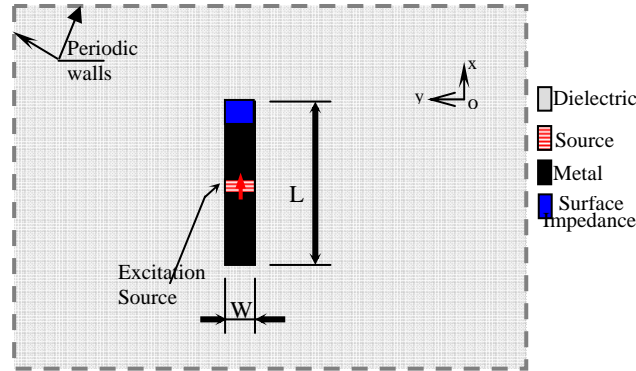


Fig. 7. Antenna Dipole studied in a case bordered of periodic walls

For the verification and the validation of simulation results, we considered an antenna dipole excited by a bilateral source along the x-axis as a test structure (Fig.7). The choice of this application, in the context of the circuit simulation bordered of periodic walls (considered to simplify the TWA), offers the possibility to define a planar source with an interrupted line. This permits to consider the artificial electric walls edging planar source, in between, the curl of the electric field will be calculated to define the voltage of the source.

The different constraints and parameters of simulation are given by table II.

TABLE II MODELING AND GEOMETRIC CONSTRAINTS

Geometric constraints
Case dimensions: a=b=6mm
Meshing: 32x32
Length of dipole: L=24/32 pixels
High of substrate: H=0.635mm
Modeling constraints
Bilateral source polarized according to x
Periodic walls
Iteration number: 300
Waveband: Fmin= 1GHz : minimal frequency Fmax= 30GHz : maximal frequency Step_Frq=0.2GHz : frequency step
Surface impedance value: Zs=0 (surface impedance sub-domain is equivalent to metallic sub-domain)
Permittivity of substrate: 9.8
$\epsilon_{r1} = 1; \epsilon_{r2} = 4.32$: permittivity of two sides

2) Yin convergence as function of iteration number

Impedance observed by the excitation source named Z_{in} (respectively the Yin admittance) is calculated to every iteration from the electromagnetic quantities, and it is major for the justification of the convergence or no of the system (equation (8)).

The figure Fig.8 proves the convergence of the TWA for almost 100 iterations for the different values of frequency. These frequencies are selected out of the resonance frequency of the dipole; otherwise, convergence is reached only after 1000 iterations since the circuit requires much energy at this frequency

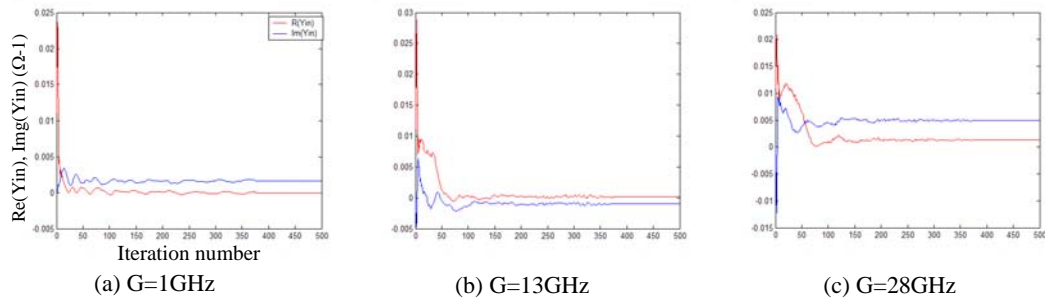


Fig. 8. Evolution of both imaginary and real part of Y_{in} , as function of iteration number for 3 frequencies (a),(b)and (c).

The algorithm of the mobile average has been applied to the TWA in order to improve the performance, while allowing the acceleration of the impedance convergence seen by the source.

3) Admittance and impedance as a function of frequency

The behaviour of Y_{in} or Z_{in} as function of frequency allows determining the resonance frequency of the studied dipole. These frequencies are in good agreement with electromagnetic theory (Fig9).

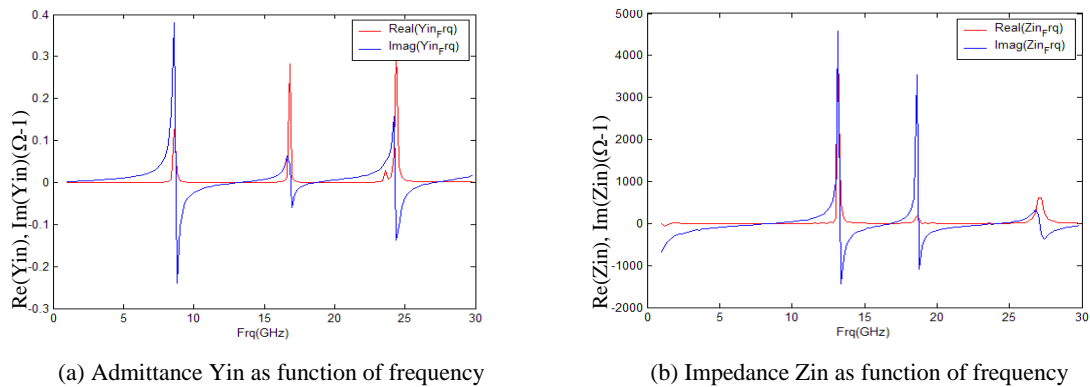


Fig. 9. Evolution of both imaginary and real part of (a) Admittance Y_{in} , (b) impedance Z_{in} as function of frequency

4) Others results

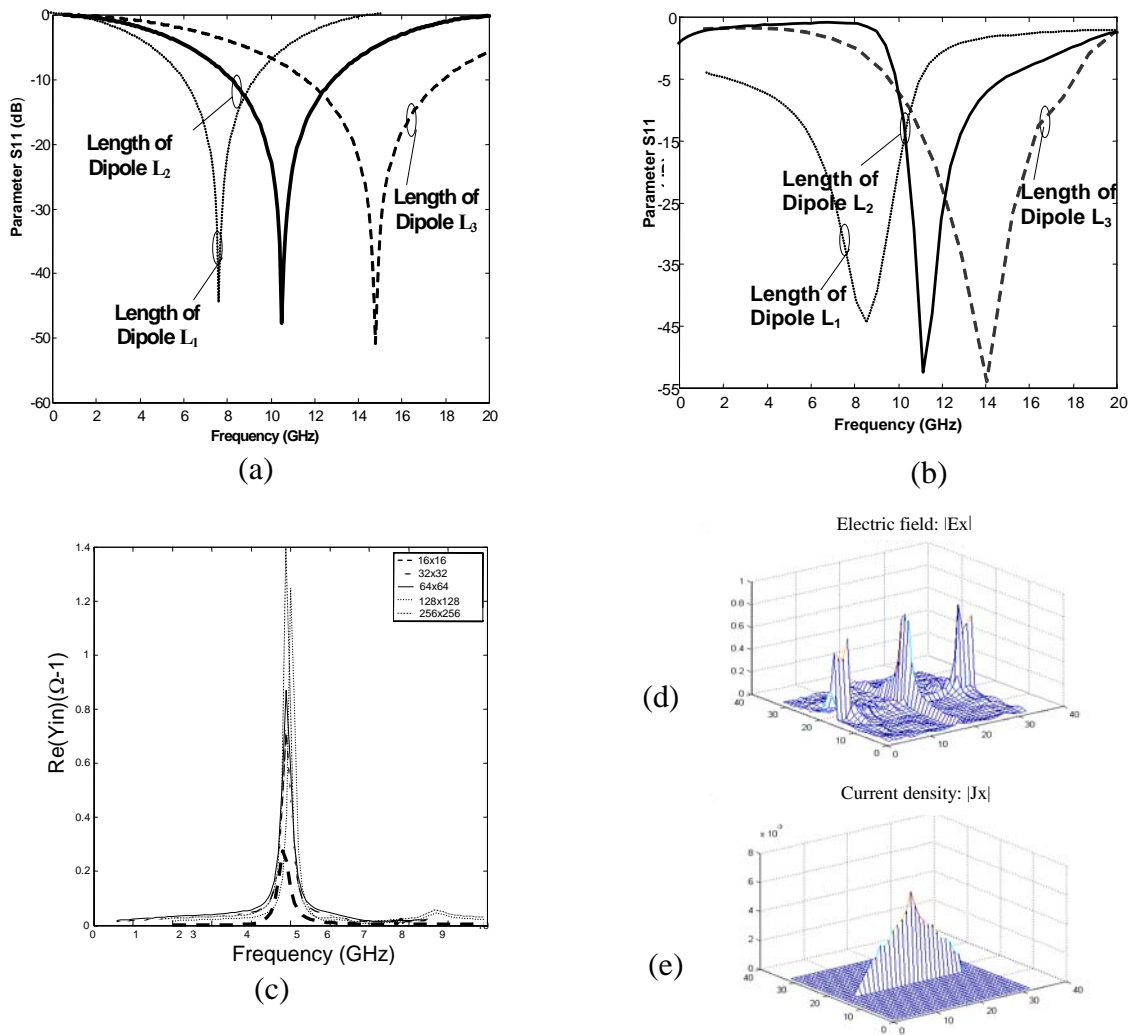


Fig. 9. (a) and (b) S11 parameter as function of frequency for 3 different lengths of dipole studied with respectively electric and periodic walls, (c) Evolution real part of Yin as function of frequency: Stability for different resolutions (16×16, 32×32, 64×64, 128×128 and 256×256), (d) and (e) Distribution of electric field and current density at 4GHz.

Figure 9 exhibits the simulation results using the parameters specified in Table II.

Indeed, the Figure 9-(b) represents the evolution of S11 parameter obtained by our electromagnetic simulation tool for three lengths of dipole: $L_1=24/32$ pixels, $L_2=20/32$ pixels, $L_3=16/32$ pixels. This result is favorably compared to the results obtained by commercial software developed under MATLAB environment [6]-[12] where the walls are electrically nature (Figure 9-(a)). Furthermore, the diminution of the length of dipole provokes an increase of resonance frequency which is in full agreement with electromagnetic theory; however, we observe some fluctuations when the dipole is near to wall what proves the influence of periodic walls [9-10].

The stability of simulation results as function of meshing resolution is verified and a good precision is appeared for high complexity problems (128×128 or 256×256) (Figure 9-(c)). The distribution of electric field and current density at 4 GHz presented, respectively, in Figure 9-(e) and (d) are satisfied

to both boundary and continuity conditions.

B. Second Application example: Sierpinski carpet

The notion of fractal geometry has become quite popular in natural sciences in recent years. Numerous research studies on fractal antennas have been proposed in the past several years [13-16]. This type of structure requires an enormous calculation above all toward the highest stages. In this context, the notion of equivalent surface impedance implemented on TWA is efficient to resolve this problem. The aim of this notion is to diminish the complex geometric intensity and reduce the CPU computation time.

For the validation of the surface impedance added to discontinuity interface, we propose to study a multi-band fractal antenna: two-stage Sierpinsky carpet while comparing the simulation result obtained by our simulation software based on TWA with two techniques: without (directly) and with surface impedance (Figure 11).

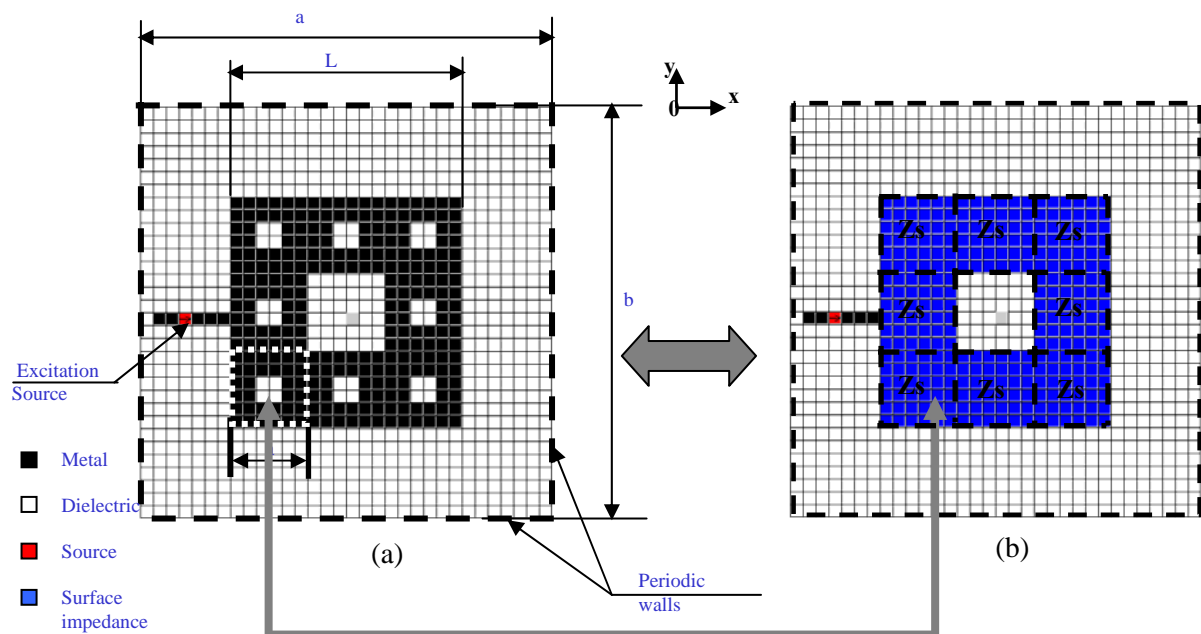


Fig. 11. Schematic of a two-stage Sierpinsky carpet (a) by direct method and (b) replaced by surface impedance ($8 \times Z_s$).

This antenna is excited by a bilateral source polarized along the x-axis. In order to avoid the problems posed by the localized sources [17], we propose to choose a source with small dimension (one pixel) and inserted to the input of metallic line.

Simulation results:

For the analysis of this antenna with the two techniques, we considered as simulation parameters those presented in the following table:

TABLE III MODELING AND GEOMETRIC CONSTRAINTS OF FRACTAL ANTENNA

Geometric constraints
Case dimensions: a=b=10mm
Meshing: 32x32
Length of antenna: L=18/32 pixels
High of substrate: H=1.52mm
Modeling constraints
Bilateral source polarized according to x
Periodic walls
Iteration number: 300
Waveband: Fmin= 1GHz : minimal frequency Fmax= 8GHz : maximal frequency Step_Frq=0.2GHz : frequency step
Permittivity of substrate: 9.8
$\epsilon_{r1} = 1; \epsilon_{r2} = 4.32$: permittivity of two sides

The TWA method offers some intrinsic potentialities to iterative process. It uncouples relations of continuities expressing boundary conditions to integral relations while taking account of half-spaces surrounding the metallic interfaces that define circuits to analyze. One of these potentialities concerns the indicatory function notion associated to the print of the circuit to study (sub-domains: metallic ‘Hm’, dielectric ‘Hi’, source ‘Hs’ and surface impedance ‘His’); the digitalization of these functions offers the possibility to analyze different scales (Fig. 12).

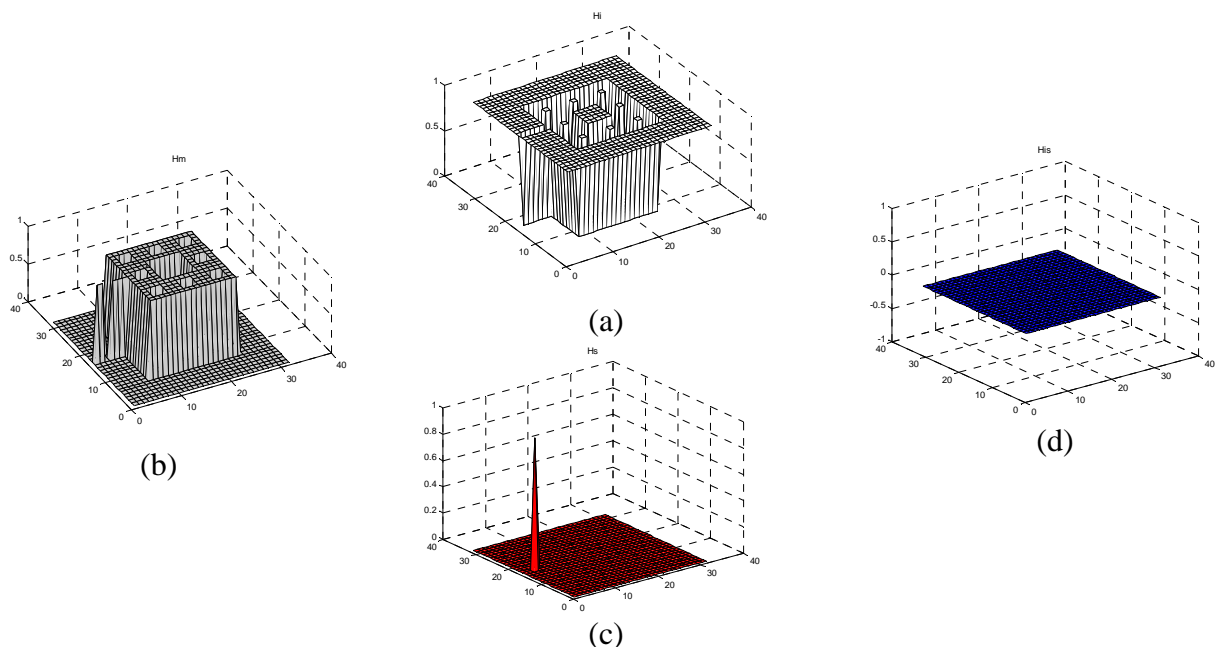


Fig. 12. Representation of indicatory functions associated to the print of a two-stage Sierpinsky carpet with the direct method (a) dielectric sub-domain: Hi ,(b) metallic sub-domain:Hm , (c)source sub-domain: Hs and (d) surface impedance sub-domain: His.

Let $Z_s=0.33i$ be the value of surface impedance correspondent to modelling constraints which was

calculated while referring on [18] and based on the renormalization method [19]. The electromagnetic simulation results of these structures (Fig.11) which were obtained using our developed software, shows clearly the correspondence between the two techniques.

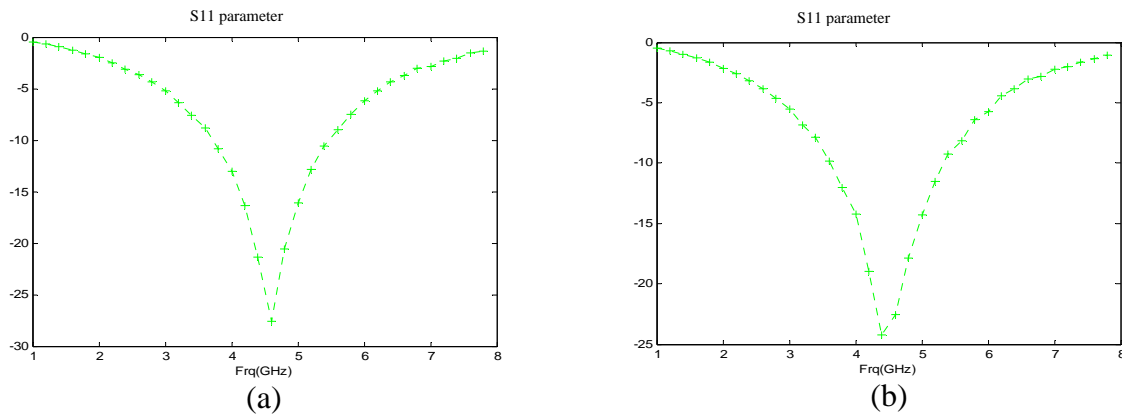


Fig. 13. Evolution of S11 parameter as a function of frequency with (a) the direct method and (b) equivalent surface impedance method.

Indeed, the values of the resonance frequency detected via the evolution S11 parameter as a function of Frequency and the input impedances Z_{in} observed by the excitation source for the two techniques (Fig.13) are analogous. Such upshot is buttressed by the relative error depicted in Table III.

TABLE III COMPARISON OF Z_{in} AT RESONANCE FREQUENCY WITH TWO TECHNIQUES

Direct technique	Surface impedance technique
F=4.577 GHz	F=4.49 GHz
Relative error: 1.90%	
$Z_{in \text{ Reduced}}(F) = 0.1329 - 0.0109i$ ($ Z_{in} = 0.1334$)	$Z_{in \text{ Reduced}}(F) = 0.1324 - 0.0125i$ ($ Z_{in} = 0.1330$)
Relative error: 0.2999%	

Moreover, the electric fields and the current densities presented respectively in figure 14 and 15 with two methods are comparable. This justifies the important role of the surface impedance notion in TWA for simplification of the complexity degree of planar circuits in a short CPU computation time.

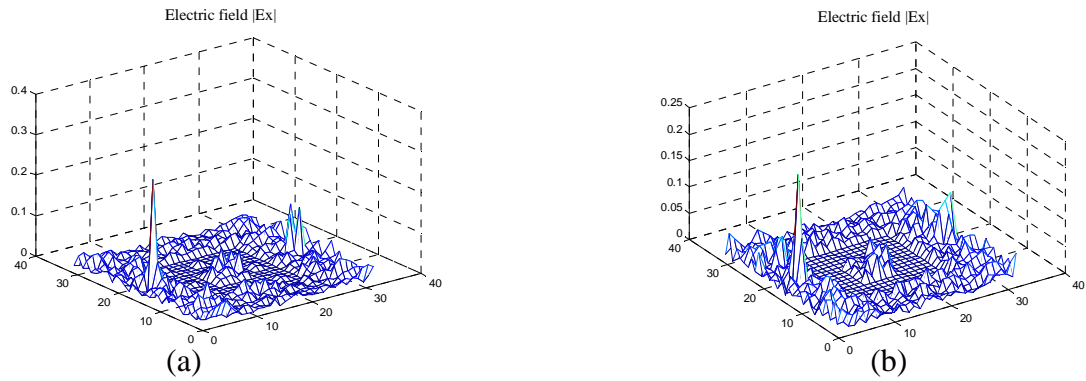


Fig. 14. Distribution of electric field at 5 GHz with (a) the direct method and (b) equivalent surface impedance method.

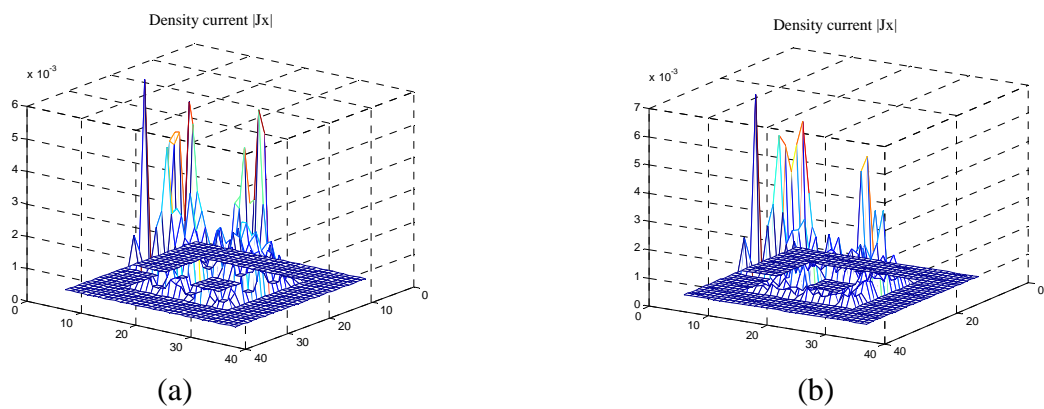


Fig. 15. . Distribution of current density at 5 GHz with (a) the direct method and (b) equivalent surface impedance method.

V. CONCLUSION

In this paper, an original integral approach based on the TWA has been presented and successfully applied to simple layer structures including the novel surface impedance sub-domain. After the validation of the surface impedance concept applied to this approach, we can go further to study planar circuits of a great compactness and a significant number of the electronic elements. However for a rigorous electromagnetic simulation with high precision, the TWA approach becomes slower because of the enormous calculation imposed by FFT. To this end, an introduction of wavelets in TWA may be a good solution to resolve this problem.

ACKNOWLEDGMENT

The authors would like to thank the reviewers for their suggestions concerning the final form of this paper.

REFERENCES

- [1] S. Wane, D. Bajon, and H. Baudrand "A new full-wave hybrid differential-integral approach for the investigation of multilayer structures" IEEE, Transactions on microwave theory and techniques, vol. 53,NO.1, January 2005.
- [2] D.Bajon,H. Baudrand; "Application of wave concept iterative Procedure(WCIP) to Planar circuits" Microtec'2000, Hanover, pp.864-868, September 2000.
- [3] D. Davidson and J.T. Aberle, "An introduction to spectral domain method-of-moments formulations," IEEE Antennas and propagation Magazine, Vol.46, No.3,June 2004
- [4] S. Mandrangeas, P. Guillon and al, "Microwave devices full-wave electromagnetic modeling using finite element method" CEFC'94, AIX les Bains, July 1994.
- [5] M.Kaddour, A. Miami and H.Baudrand" Analysis of multilayer microstrip antennas by using iterative method" Journal of Microwaves and optoelectronics Vol 3 No.1, April 2003.
- [6] S. Wane " contribution à la modélisation électromagnétique des circuits intégrés multicouches : Réalisation d'un logiciel de simulation et d'aide à la conception des stratégies d'isolation" Thèse de doctorat de l'INPT-Toulouse France Année 2002.
- [7] M. Titaouine, A. Neto, and H. Baudrand "A WCIP method applied to active frequency selective surfaces" Journal of microwave and optoelectronics vol. 6, No.1, June 2007.
- [8] M. Ayari, T. Aguilí, H.Baudrand "An electromagnetic simulation tool based on the original Transverse Wave Approach (TWA)" WorldComp'07,Las Vegas, Nevada, USA, MSV7410 ,June 2007.
- [9] M.Ayari, T. Aguilí, H.Baudrand; "Implémentation de l'approche itérative sous l'environnement orienté objet visual c++: Application à l'étude des couplages entre antennes dipôles " ISESC'05,Jijel, Algeria pp.145-149, Part I. ,June 2005.
- [10] M.Ayari, T. Aguilí, H.Baudrand; "Implémentation de l'approche en ondes transverses sous l'environnement c++: Applications aux antennes dipôles en réseaux périodiques " SETIT'04, Sousse, Tunisia pp.281, March 2004.
- [11] R.F.Remis, P.van den Berg "A modified Lanczos Algorithm for the Computation of transient Electromagnetic Wave fields" IEEE, Transactions on microwave theory and techniques, vol. 45, NO.12, Dec 1997.
- [12] D.Bajon, S. Wanne and H. Baudrand « Développement d'outils de simulation électromagnétique et de conception de circuits radiofréquences et antennes » Physique-RSTD 63, pp.109-121, March 2004.
- [13] D. Voyer, H. Aubert and H. Baudrand "Analyse électromagnétique récursive pour le calcul de l'impédance des iris fractals" 13^{ème} Journées Nationale Micro Ondes, France May 2003.
- [14] S. R. Best "A comparison of the performance proprieties of the Hilbert Curve Fractal and Meander Line monopole antennas" Microwave and optical technology letters, vol.35,N°4, November 2002.
- [15] C. Tricot "Curves and fractal dimension", Springer-Verlag, New York, 1995.
- [16] Bin Lin and Z. R. Yang "A suggested lacunarity expression for Sierpinski carpets" J. Phys.A: Math. Gen 19, L49-L52, 1986.
- [17] K.Grayaa, N. Hamdi, T. Aguilí and A. Bouallegue; 'Full-wave analysis of shielded planar circuits using different models of sources', IEE Proc.- Microw. Antennas Propag., Vol. 150, August 2003,pp.258-264.
- [18] T. Aguilí and T. Ben salah "Etude d'une structure fractale multi-échelle en utilisant le modèle du multi-port" OHD'05, Hammamet- Tunis pp. 184-187, September 2005.
- [19] C. Arbi and A. Bouallegue "Etude des caractéristiques de rayonnement d'une antenne fractale par la norme de renormalisation" OHD'05, Hammamet- Tunis pp. 184-187, September 2005